Random-phase-approximation correlation method including exchange interactions

Andreas Heßelmann

Lehrstuhl für Theoretische Chemie, Universität Erlangen-Nürnberg and Egerlandstrasse 3, D-91058 Erlangen, Germany

(Received 1 December 2011; published 25 January 2012)

Two random-phase-approximation correlation methods are introduced that take into account exchange interactions. The first one, termed RPAX, is obtained from a simple modification of the ring coupled-cluster doubles amplitude equation, while the second, termed RPAX2, is based on the first method using a slightly modified update equation for the amplitudes. It is shown that this second RPAX2 method can be implemented with a computational algorithm that scales only with the fifth power of the molecular size with the aid of density fitting or the Cholesky decomposition of two-electron integrals. It is thus not much more costly than standard second-order perturbation theory methods and can be applied to quite large molecular systems. Moreover, numerical tests for chemical reaction energies and intermolecular interaction energies have shown that the RPAX2 method, if based on a Perdew-Burke-Ernzerhof exchange Kohn-Sham reference determinant, yields results which are very close to coupled-cluster with single, double, and perturbative triple excitations reference results.

DOI: 10.1103/PhysRevA.85.012517 PACS number(s): 31.10.+z, 31.15.−p, 34.20.Gj, 34.50.Lf

I. INTRODUCTION

The direct random-phase approximation (dRPA) describes electron correlation effects by summing over all particle-hole interactions [1]. This leads to the so-called ring approximation as the corresponding correlation energy contributions are represented by corresponding ring diagrams in a perturbation expansion. It turns out that in the limit of a high-density electron gas, these ring diagrams represent the most important contributions to the correlation energy [1]. Thus, it can be expected that the dRPA method performs well for bulk systems while its performance deteriorates for describing electron correlation in molecules. In fact, some recent studies have shown that the dRPA correlation energies strongly overestimate the correlation energies from accurate reference methods for a number of atoms and molecules [2–4]. The reason for this, in analogy to the first-order case if only Coulomb interactions are accounted for (Hartree method), is that the dRPA correlation energy contains correlation interactions of the electrons with themselves that are not corrected. These higher-order self-correlation terms, however, can be removed if exchange effects are accounted for in the infinite-order summation of particle-hole interaction terms.

There is no unique way to account for electron exchange in RPA methods, and a number of approaches have been developed [5–11], the most early one perhaps being the ring coupled-cluster doubles method from McLachlan and Ball (see also a recent review about RPA exchange methods based on both Hartree-Fock and Kohn-Sham reference determinants [4]). It turns out, however, that in contrast to, for example, second-order Møller-Plesset perturbation theory methods or not much more computationally expensive coupled-cluster methods, some of these RPA exchange methods are not very accurate in describing the ground states of molecules [3,4]. A recent study of Hartree-Fock-based RPA methods has shown that this can be attributed to a large over- or underestimation of third-order correlation effects occurring in these methods, stemming from neglected particle-particle and hole-hole interaction terms, which are not accounted for in "normal" RPA methods (they are described in so-called higher-order RPA variants such as the second-order polarization propagator approximation (SOPPA) [3,9,12]. A simple correction method for the third-order correlation contribution has led to a strong improvement for both total energies and energy differences, namely reaction energies and intermolecular interaction energies, for these methods [3].

Another way to improve upon RPA methods is to combine RPA with [4,11,13] or without [14,15] exchange using Kohn-Sham instead of Hartree-Fock reference determinants. It was found in recent works that in the dRPA case this approach leads to fairly good atomization energies compared to standard density functional theory (DFT) methods [14] and even is able to describe the dissociation of chemical triple bonds [14], the latter being a very difficult case for standard single-reference correlation methods. A study by Kresse *et al.* has shown that the dRPA method yields excellent lattice constants and good relative energies for a set of 24 solids [16]. However, though dRPA methods describe van der Waals interactions qualitatively correctly, Kohn-Sham-based dRPA methods fail to deliver an accuracy at least comparable to MP2 theory for weak intermolecular interactions [13,17].

One approach to improve on Kohn-Sham dRPA methods for intermolecular interactions is to combine dRPA [18,19] or RPA including exchange effects [13,20,21] with standard density functional methods for describing the short-range electron-electron interactions using a range separation of the Coulomb interaction operator. These range-separated DFT-RPA methods not only were shown to yield accurate intermolecular interaction energies [13,19] but also reduce the unfavorable basis set dependence of standard RPA methods as the interelectronic cusp does not need to be described (explicitly) in range-separated DFT-RPA.

Another recently developed exchange RPA method, termed EXX-RPA, is based on the adiabatic-connection fluctuation-dissipation theorem and takes exchange effects into account using the nonadiabatic and frequency-dependent exact exchange DFT kernel [2,4,22–24]. While this method so far has not been tested for weak intermolecular interactions, it yields fairly good atomic energies [2] and chemical reaction

energies [23] and describes the dissociation of molecular pair bonds correctly [24]; that is, it gives a good description of static electron correlation effects in contrast to perturbation theory methods, for example.

A main problem of current Kohn-Sham-based RPA methods that contain exchange interactions is that, apart from the interelectronic cusp problem, the total scaling behavior with respect to the molecular size is much larger than with common DFT methods. Since RPA exchange methods can be categorized as coupled-cluster doubles (CCD) methods that exclude ladder diagrams [25,26], also their scaling behavior is the same as for CCD, that is, $\mathcal{N}^6$ with $\mathcal{N}$ denoting a measure for the molecular size. This is one order of magnitude larger than with second-order perturbation theory correlation methods and even between one and two orders of magnitude larger than with dRPA [27]. Therefore, such RPA exchange methods soon become impractical for larger molecular systems. A remedy to this problem has been derived by Kresse *et al.*, who contract the amplitudes from the direct ring CCD equation with antisymmetrized integrals to obtain the correlation energy [11]. This method, termed second-order screened exchange (SOSEX), is exact to the second order of perturbation theory and scales only with the fifth power of $\mathcal{N}$, thus having a similar computational expense as MP2. While it has been shown that SOSEX improves the dRPA method for atomization energies and lattice constants [11], a recent study of chemical reaction energies has shown that the SOSEX method is not much more accurate than MP2 [4].

In this work, a new Kohn-Sham-based RPA method with exchange interactions is introduced which also scales only with the fifth power of the molecular size and at the same time yields very accurate reaction energies and intermolecular interaction energies. As this method is based on a computational efficient update scheme for the amplitudes that first was derived for the dRPA case, in Sec. II A, a corresponding approach is presented for the dRPA case. Then, in Sec. II B, two new RPA methods, termed RPAX and RPAX2, are introduced that are both based on a modified ring CCD equation. The first method, RPAX, can not be implemented with an $\mathcal{N}^5$ scaling and does not perform much better than MP2 for a set of chemical reactions; see Sec. IV C. In contrast to this, the second method, termed RPAX2, not only scales with $\mathcal{N}^5$ but even yields reaction energies and intermolecular interaction energies that are in fairly good agreement with high-level coupled-cluster singles doubles with perturbative triples (CCSD(T)) values; see Secs. IV C and IV D. General technical details of this method are presented in Sec. III while in Sec. IV A the accuracy of the density fitting and Cholesky decomposition approaches required to achieve an $\mathcal{N}^5$ scaling is analyzed. Section V summarizes the results.

II. METHOD

A. Efficient implementation of the direct RPA method

The dRPA correlation energy can be obtained from the equation [26,28]

$$E_c^{\mathrm{dRPA}} = \tfrac{1}{2}\mathrm{Tr}(\mathbf{CT}), \tag{1}$$

where $C_{ia,jb} = [ia|jb]$ is a two-electron repulsion integral (in chemist's notation) using combined indices of occupied (i,j) and virtual spin-orbital indices (a,b) and $\mathbf{T}$ are double excitation amplitudes that can be obtained from the solution of the Riccati equation [26,29]

$$\begin{aligned}&\mathbf{C} + \boldsymbol{\varepsilon}\mathbf{T} + \mathbf{T}\boldsymbol{\varepsilon} + \mathbf{CT} + \mathbf{TC} + \mathbf{TCT}\\ &\quad = \boldsymbol{\varepsilon}\mathbf{T} + \mathbf{T}\boldsymbol{\varepsilon} + (\mathbf{1}+\mathbf{T})\mathbf{C}(\mathbf{1}+\mathbf{T}) = \mathbf{0},\end{aligned} \tag{2}$$

where $\boldsymbol{\varepsilon}$ is a diagonal matrix containing the orbital energy differences $\varepsilon_a - \varepsilon_i$ in its diagonal. Equation (2) can be solved through an iterative update of the amplitudes by using

$$\mathbf{T}^{(n+1)} = -\boldsymbol{\Delta} \circ (\mathbf{C} + \mathbf{CT}^{(n)} + \mathbf{T}^{(n)}\mathbf{C} + \mathbf{T}^{(n)}\mathbf{CT}^{(n)}), \tag{3}$$

where n denotes the current cycle of the iterative process and the operator $\circ$ here defines an entrywise matrix product (Hadamard product). The matrix $\boldsymbol{\Delta}$ is defined by the matrix elements $\Delta_{ia,jb} = 1/(\varepsilon_a - \varepsilon_i + \varepsilon_b - \varepsilon_j)$ with the orbital energies $\varepsilon_i, \varepsilon_j$ corresponding to the occupied orbitals ϕ_i and ϕ_j and the orbital energies $\varepsilon_a, \varepsilon_b$ corresponding to the unoccupied orbitals ϕ_a and ϕ_b. The iteration of Eq. (3) can be initialized with $\mathbf{T}^{(0)} = \mathbf{0}$, yielding $\mathbf{T}^{(1)} = -\boldsymbol{\Delta} \circ \mathbf{C}$ in the first cycle. As the matrix products in Eq. (3) scale as $(N_{\mathrm{occ}} N_{\mathrm{virt}})^3$ with N_{occ} and N_{virt} being the number of occupied and unoccupied orbitals, respectively, the direct implementation of Eq. (3) leads to an overall scaling behavior of $\mathcal{N}^6$ with the molecular size $\mathcal{N}$, and thus the expense would be prohibitively large. However, this scaling behavior can be reduced by two orders of magnitude if the matrix $\mathbf{C}$, which is positive definite, is decomposed using its Cholesky decomposition [30,31]

$$\mathbf{C} = \mathbf{LL}^T \tag{4}$$

with $\mathbf{L}$ being a triangular matrix containing the Cholesky vectors in its columns or similarly by using density fitting [32–34]

$$\mathbf{C} = (\mathbf{NS}^{-1/2})(\mathbf{NS}^{-1/2})^T = \mathbf{LL}^T, \tag{5}$$

where $\mathbf{N}$ is a three-index Coulomb repulsion integral defined by the matrix elements $N_{ia,P} = [ia|P]$ with P denoting an auxiliary basis function index [note that the matrices $\mathbf{L}$ differ in Eqs. (4) and (5)]. The matrix $\mathbf{S}$ is an overlap matrix in the auxiliary function space. The crucial point is now that either the number of Cholesky vectors or the number of auxiliary basis functions required to approximate the matrix $\mathbf{C}$ via Eqs. (4) or (5) will only scale linearly with the system size. Correspondingly, the positive definite matrix $\boldsymbol{\Delta}$ can be decomposed using the Cholesky decomposition

$$\boldsymbol{\Delta} = \boldsymbol{\epsilon}\boldsymbol{\epsilon}^T = \sum_{\omega}^{N_\omega} \epsilon_{ia,\omega}\epsilon_{jb,\omega} = \sum_{\omega} \mathbf{e}_\omega \mathbf{e}_\omega^T \tag{6}$$

with ω denoting the index of the Cholesky vector and $\mathbf{e}_\omega$ representing the corresponding Cholesky vector. In Ref. [35], it has been shown that the Cholesky decomposition of energy denominators is size intensive; that is, for two identical noninteracting systems the number of Cholesky vectors required to obtain the matrix $\boldsymbol{\Delta}$ with a given precision is identical to the number of Cholesky vectors required for one subsystem. Moreover, even for quite large systems the number of Cholesky vectors required to achieve a precision of the denominator matrix elements of 10^{-8} ranges between 10 and 15 and so it can be assumed that it is almost independent of the system size.

The insertion of Eqs. (4) or (5) and Eq. (6) into Eq. (3) leads to the following efficient update formula for the amplitudes:

$$\mathbf{T}^{(n+1)} = -\sum_{\omega} \mathbf{e}_{\omega} \cdot (\mathbf{L} + \mathbf{T}^{(n)}\mathbf{L})(\mathbf{L} + \mathbf{T}^{(n)}\mathbf{L})^{T} \cdot \mathbf{e}_{\omega}^{T}, \quad (7)$$

where the center dots are introduced to define the products $(\mathbf{a} \cdot \mathbf{b})_{ij} = a_i b_{ij}$ between a vector $\mathbf{a}$ and a matrix $\mathbf{b}$. Equation (7) shows that in each cycle of the iteration the amplitudes can be written in the form

$$\mathbf{T}^{(n+1)} = -\sum_{\omega} \mathbf{e}_{\omega} \cdot \mathbf{U}^{(n)}\mathbf{U}^{(n)T} \cdot \mathbf{e}_{\omega}^{T} \quad (8)$$

with $\mathbf{U}^{(n)} = \mathbf{L} + \mathbf{T}^{(n)}\mathbf{L}$ so that instead of updating the full four-index amplitudes it is sufficient to update the three-index matrix $\mathbf{U}$ that has $N_{\mathrm{occ}} \times N_{\mathrm{virt}}$ rows and N_{chol} or N_{aux} columns, depending on whether the decomposition of Eqs. (4) or (5) is used. It can easily be verified that this requires only matrix products that scale as $N_{\mathrm{occ}} N_{\mathrm{virt}} N_{\mathrm{chol}}^2$ or $N_{\mathrm{occ}} N_{\mathrm{virt}} N_{\mathrm{aux}}^2$ and thus is an $\mathcal{N}^4$ scaling process. Using Eqs. (4), (5), and (8), the correlation energy can be obtained by

$$E_{\mathrm{c}}^{\mathrm{dRPA}} = \frac{1}{2} \sum_{\omega} \mathrm{Tr}[(\mathbf{L}^{T}\mathbf{e}_{\omega} \cdot \mathbf{U})(\mathbf{L}^{T}\mathbf{e}_{\omega} \cdot \mathbf{U})^{T}], \quad (9)$$

which too can be computed with $\mathcal{N}^4$ scaling. In the next section, it is shown that a very similar scheme is also possible if electron exchange effects are accounted for; however, that leads to a scaling behavior that is one order of magnitude larger than for dRPA.

B. RPA method with exchange interactions

There exists no unique way to include exchange effects in RPA methods, and a number of different approaches have been derived in the past [5–11]. The most simple way to account for electron exchange is to contract the dRPA amplitudes (denoted hereafter as $\mathbf{T}^{\mathrm{dRPA}}$) from Eq. (2) with antisymmetrized two-electron integrals, which are defined here as $B_{ia,jb} = [ia|jb] - [ib|ja] = C_{ia,jb} - \hat{P}_{ab} C_{ia,jb} = C_{ia,jb} - K_{ia,jb}$, where $\hat{P}_{ab}$ is a permutation operator that permutes the orbitals with indices a and b. This yields

$$E_{\mathrm{c}}^{\mathrm{SOSEX}} = \tfrac{1}{2}\mathrm{Tr}(\mathbf{B}\mathbf{T}^{\mathrm{dRPA}}), \quad (10)$$

which is termed as second-order screened exchange (SOSEX) correlation energy [11]. It can be shown that SOSEX is exact to second order [28] (if singles contributions are neglected); that is, the correlation energy contribution to second order in the electron-electron interaction is given by $E_{\mathrm{c}}^{(2)} = -\frac{1}{2}\mathrm{Tr}(\mathbf{C}\mathbf{B} \circ \mathbf{\Delta})$. In third and higher orders, however, the correction of the self-correlation error which occurs in dRPA is incomplete [3,4]. A more effective way to include the self-correlation correction in RPA that is proposed here is to use antisymmetrized two-electron integrals in the Riccati equation (2), which then is written as

$$\begin{aligned} &\mathbf{B} + \boldsymbol{\varepsilon}\mathbf{T} + \mathbf{T}\boldsymbol{\varepsilon} + \mathbf{B}\mathbf{T} + \mathbf{T}\mathbf{B} + \mathbf{T}\mathbf{B}\mathbf{T} \\ &\quad = \boldsymbol{\varepsilon}\mathbf{T} + \mathbf{T}\boldsymbol{\varepsilon} + (\mathbf{1} + \mathbf{T})\mathbf{B}(\mathbf{1} + \mathbf{T}) = \mathbf{0}. \end{aligned} \quad (11)$$

Note that this equation differs from the ring coupled-cluster doubles equation [26] in which the linear terms in the amplitudes are contracted with the integrals $A_{ia,jb} = [ia|jb] - [ij|ab]$. A justification for using Eq. (11) instead of the ring coupled-cluster doubles equation is that it can easily be verified that for a two-electron system, for which $\mathbf{B} = \frac{1}{2}\mathbf{C}$ holds true, the approach will be identical to the EXX-RPA method (if an exact-exchange Kohn-Sham reference determinant is used), which has been shown to accurately describe both the static and the dynamic correlation contributions of two-electron systems [2,24]. The correlation energy of this approach, termed as RPAX here, is then given as

$$E_{\mathrm{c}}^{\mathrm{RPAX}} = \tfrac{1}{2}\mathrm{Tr}(\mathbf{C}\mathbf{T}^{\mathrm{RPAX}}) \quad (12)$$

and has thus the same form as for dRPA [Eq. (1)] but with the amplitudes $\mathbf{T}^{\mathrm{RPAX}}$ stemming from the solution of Eq. (11) instead of Eq. (2).

We now seek an efficient implementation of the RPAX method similar to the scheme used for dRPA presented in Sec. II A. For this, the Riccati equation (11) is transformed to an iterative update formula for the amplitudes

$$\begin{aligned} \mathbf{T}^{(n+1)} &= -\mathbf{\Delta} \circ [(\mathbf{1} + \mathbf{T}^{(n)})\mathbf{B}(\mathbf{1} + \mathbf{T}^{(n)})] \\ &= -\mathbf{\Delta} \circ [(\mathbf{1} + \mathbf{T}^{(n)})\mathbf{C}(\mathbf{1} + \mathbf{T}^{(n)}) \\ &\quad - (\mathbf{1} + \mathbf{T}^{(n)})\mathbf{K}(\mathbf{1} + \mathbf{T}^{(n)})] \quad (13) \\ &= -\mathbf{\Delta} \circ [(\mathbf{1} + \mathbf{T}^{(n)})\mathbf{C}(\mathbf{1} + \mathbf{T}^{(n)}) \\ &\quad - (\mathbf{1} + \mathbf{T}^{(n)})\hat{P}\mathbf{C}(\mathbf{1} + \mathbf{T}^{(n)})]. \quad (14) \end{aligned}$$

Equation (14) is identical to Eq. (7) with exception of the antisymmetrized second term in the brackets in Eq. (14). If the iteration is initialized with $\mathbf{T}^{(0)} = \mathbf{0}$, then the amplitudes of the first iteration cycle are given by

$$\mathbf{T}^{(1)} = -\mathbf{\Delta} \circ (\mathbf{C} - \hat{P}\mathbf{C}) = -\mathbf{\Delta} \circ (\mathbf{L}\mathbf{L}^{T} - \hat{P}\mathbf{L}\mathbf{L}^{T}), \quad (15)$$

where the decompositions of Eqs. (4) or (5) for the matrix $\mathbf{C}$ were used. In order to arrive at a computationally efficient scheme, Eq. (14) is slightly modified by moving the antisymmetrization operator $\hat{P}$ to the front of the second term within the parentheses, yielding

$$\begin{aligned} \mathbf{T}^{(n+1)} &= -\mathbf{\Delta} \circ [(\mathbf{1} + \mathbf{T}^{(n)})\mathbf{C}(\mathbf{1} + \mathbf{T}^{(n)}) \\ &\quad - \hat{P}(\mathbf{1} + \mathbf{T}^{(n)})\mathbf{C}(\mathbf{1} + \mathbf{T}^{(n)})], \end{aligned} \quad (16)$$

which now has the same structure as Eq. (15). Using the decompositions (4) or (5) of the matrix $\mathbf{C}$, the amplitudes iteration can therefore be written as

$$\mathbf{T}^{(n+1)} = -\mathbf{\Delta} \circ [\mathbf{U}^{(n)}\mathbf{U}^{(n)T} - \hat{P}\mathbf{U}^{(n)}\mathbf{U}^{(n)T}] \quad (17)$$

with $\mathbf{U}^{(n)} = \mathbf{L} + \mathbf{T}^{(n)}\mathbf{L}$. Similar to the the dRPA case [see Eq. (8)], it is therefore sufficient to iterate on the three-index matrix $\mathbf{U}$ with the dimension $N_{\mathrm{occ}} \times N_{\mathrm{virt}} \times N_{\mathrm{aux}}$ instead of the full four-index amplitudes $\mathbf{T}$. Explicitly, the update equation for $\mathbf{U}$ is given by

$$\mathbf{U}^{(n+1)} = \mathbf{L} + \mathbf{T}^{(n)}\mathbf{L} \quad (18)$$

with $\mathbf{T}^{(n)}$ computed from the matrix $\mathbf{U}^{(n)}$ of the previous cycle using Eq. (17). It can be seen that this iteration process requires at most operations that scale as $N_{\mathrm{occ}}^2 N_{\mathrm{virt}}^2 N_{\mathrm{aux}}$ and therefore has a total scaling behavior of $\mathcal{N}^5$ with the molecular size $\mathcal{N}$. The correlation energy can be obtained by

$$E_{\mathrm{c}}^{\mathrm{RPAX2}} = \tfrac{1}{2}\mathrm{Tr}(\mathbf{L}^{T}\mathbf{T}^{(\infty)}\mathbf{L}), \quad (19)$$

which scales as $\mathcal{N}^5$ with the aid of Eq. (17) and $\mathbf{T}^{(\infty)}$ represents the solution to Eqs. (16) or (17), respectively. As the correlation energy of Eq. (19) will differ from the RPAX correlation energy of Eq. (12), due to the modification made in Eq. (16), this second approach is termed as RPAX2 here. The RPAX2 method itself is again exact to second order but differs from RPAX in third and higher orders. Using the definition $\mathbf{\Delta} \circ \mathbf{M} = \overline{\mathbf{M}}$ for a general matrix $\mathbf{M}$ with the dimension $N_{\mathrm{occ}} \times N_{\mathrm{virt}}$ and $\mathbf{K} = \hat{P}\mathbf{C}$, the third-order energy of the RPAX approach is given by

$$E_{\mathrm{c}}^{(3)}[\mathrm{RPAX}] = \mathrm{Tr}[\overline{\mathbf{C}}\mathbf{C}\overline{\mathbf{C}}] - \tfrac{1}{2}\mathrm{Tr}[\overline{\mathbf{K}}\mathbf{C}\overline{\mathbf{C}}] - \tfrac{1}{2}\mathrm{Tr}[\overline{\mathbf{C}}\mathbf{C}\overline{\mathbf{K}}] - \mathrm{Tr}[\overline{\mathbf{C}}\mathbf{K}\overline{\mathbf{C}}] + \tfrac{1}{2}\mathrm{Tr}[\overline{\mathbf{K}}\mathbf{K}\overline{\mathbf{C}}] + \tfrac{1}{2}\mathrm{Tr}[\overline{\mathbf{C}}\mathbf{K}\overline{\mathbf{K}}], \tag{20}$$

while in case of the RPAX2 approach it is given by

$$E_{\mathrm{c}}^{(3)}[\mathrm{RPAX2}] = \mathrm{Tr}[\overline{\mathbf{C}}\mathbf{C}\overline{\mathbf{C}}] - \mathrm{Tr}[\overline{\mathbf{K}}\mathbf{C}\overline{\mathbf{C}}] - \mathrm{Tr}[\overline{\mathbf{C}}\mathbf{C}\overline{\mathbf{K}}] + \mathrm{Tr}[\overline{\mathbf{K}}\mathbf{C}\overline{\mathbf{K}}]. \tag{21}$$

It can be seen that the last three terms in Eq. (20) are improper third-order contributions as they do not correspond to terms appearing in third-order of perturbation theory. The reason for this is that the corresponding perturbation theory diagrams contain interaction vertices with two incoming fermion lines on one side so that it is impossible to draw a closed loop for it, and thus it violates one of the rules for Feynman diagrams [25]. On the other hand, the third-order terms appearing in the RPAX2 correlation energy shown in Eq. (21) are all proper third-order contributions, and their diagrammatic representation is displayed in Fig. 1. It can thus be seen that the modification of Eq. (14), which was motivated by gaining a higher efficiency of the method, also leads to a theoretically more justified approach, in contrast to the RPAX method. In Sec. IV, we investigate how the RPAX and RPAX2 methods differ from each other with respect to their total energies and reaction energies for a number of small organic molecules.

So far, the descriptions of the reference state and single excitations have been omitted. Since the RPA method here is presented as a wave function method, it seems reasonable to describe single excitations in very much the same way as is done in related coupled-cluster methods; that is, in addition to Eqs. (14) or (16), it is possible to derive equations for single excitation amplitudes. However, while this might be useful in Hartree-Fock-based RPA methods, in Kohn-Sham-based RPA approaches (i.e., RPA approaches that use Kohn-Sham reference determinants) this would lead to some redundancies in the description of single excitations. The reason for this is that the Kohn-Sham determinant (obtained from approximate exchange-correlation potentials) is close to the Brueckner determinant from a Brueckner coupled-cluster doubles (BCCD) wave function [36]. In BCCD, singles do not appear but they are "absorbed" into the reference determinant by an occupied-virtual unitary transformation [37]. Therefore, in this work an explicit description of single excitations is omitted, and the reference determinant Φ is calculated using Kohn-Sham DFT. The total energy of the RPAX and RPAX2 method is then calculated by

$$E^{\mathrm{RPAX,RPAX2}} = \langle \Phi^{\mathrm{KS}} | \hat{H} | \Phi^{\mathrm{KS}} \rangle + E_{\mathrm{c}}^{\mathrm{RPAX,RPAX2}}, \tag{22}$$

where $\hat{H}$ is the Hamilton operator and $E_{\mathrm{c}}^{\mathrm{RPAX,RPAX2}}$ is defined in Eqs. (12) and (19). It has been observed that in the case of intermolecular interactions, in particular, the performance of the RPAX and RPAX2 method depends on the choice of the exchange-correlation functional used to calculate the Kohn-Sham orbitals. A few examples for this are shown in Sec. IV C. It was found that a very accurate description, both for reaction energies and intermolecular interactions, is achieved if the reference determinant is calculated using the Perdew-Burke-Ernzerhof exchange (PBEx) functional [38]; see Sec. IV for numerical results.

III. COMPUTATIONAL DETAILS

The RPAX and RPAX2 methods described in Sec. II B were tested for a set of 16 chemical reaction energies of some small organic molecules shown in Table I and for the 22 intermolecular complexes from the S22 database developed by Hobza *et al.* [39] for studying the performance for intermolecular interaction energies. In the case of the set of chemical reactions the molecular geometries were taken from Ref. [40], while in the case of the S22 systems the geometries were taken from Ref. [39]. While the S22 database contains complexes that are in their equilibrium structure, for two systems from the S22 database, namely the ethyne-ethene and the ethene dimer, also the interaction energies at nonequilibrium distances have been studied by decreasing and increasing the distance of the centers of mass in both cases relative to their equilibrium structures.

The RPAX and RPAX2 methods have been implemented using the amplitude update Eqs. (14) and (16), respectively. It turned out that a simple damping scheme using

$$\widetilde{\mathbf{T}}^{(n+1)} = (1-n)\mathbf{T}^{(n+1)} + n\mathbf{T}^{(n)} \tag{23}$$

with $n = 0.4$ is sufficient to achieve a convergence of the energy of 10^{-8} Hartree to within 10 to 20 iteration cycles. The same scheme with a mixture of 40% of the $\mathbf{U}$ matrix from the previous cycle has also been used for the density-fitting respectively Cholesky decomposition approach for the RPAX2 method using the update Eqs. (17) and (18). It was found that with this, for a given system, the density fitting and Cholesky decomposition approach even converged more rapidly than the iteration on the full amplitudes.

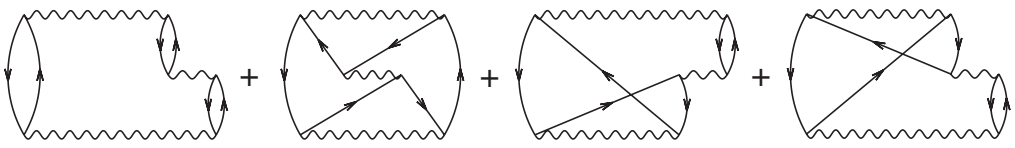

FIG. 1. Third-order Goldstone diagrams that represent the third-order correlation energy contribution to the RPAX2 correlation energy.

TABLE I. Reaction energies for 16 chemical reactions (in kcal/mol). The mean absolute errors (mae) and relative deviations ($|\Delta|$) to the CCSD(T) reference values are shown in the last two lines of the table.

Reaction	MP2	CCSD	CCSD(T)	RPAX	RPAX2
$C_2H_2+H_2\rightarrow C_2H_4$	−47.16	−50.46	−49.44	−51.69	−49.39
$C_2H_4+H_2\rightarrow C_2H_6$	−40.86	−40.49	−39.47	−40.70	−39.40
$C_2H_6+H_2\rightarrow 2CH_4$	−17.73	−18.76	−18.18	−18.35	−18.42
$CO+H_2\rightarrow HCHO$	−5.94	−5.61	−5.47	−4.62	−4.00
$HCHO+H_2\rightarrow CH_3OH$	−30.15	−30.78	−29.70	−31.63	−29.31
$H_2O_2+H_2\rightarrow 2H_2O$	−91.98	−89.55	−87.63	−89.79	−87.97
$C_2H_2+H_2O\rightarrow CH_3CHO$	−36.41	−38.53	−38.28	−39.65	−38.02
$C_2H_4+H_2O\rightarrow C_2H_5OH$	−14.86	−14.43	−14.12	−15.17	−13.67
$CH_3CHO+H_2\rightarrow C_2H_5OH$	−25.60	−26.36	−25.28	−27.21	−25.05
$CO+NH_3\rightarrow HCONH_2$	−12.23	−9.35	−10.26	−9.57	−8.57
$CO+H_2O\rightarrow CO_2+H_2$	−10.02	−3.76	−6.18	−4.30	−5.36
$HNCO+NH_3\rightarrow NH_2CONH_2$	−19.28	−22.04	−20.70	−22.62	−19.59
$CO+CH_3OH\rightarrow HCOOCH_3$	−15.19	−12.12	−13.59	−12.62	−11.93
$HCOOH+NH_3\rightarrow HCONH_2+H_2O$	−2.03	−1.24	−1.16	−1.42	−1.25
$CO+H_2O\rightarrow CO_2+H_2O$	−102.00	−93.31	−93.81	−94.09	−93.33
$H_2CCO+HCHO\rightarrow C_2H_4O+CO$	−3.12	−4.93	−3.83	−5.92	−3.91
mae	1.93	0.95		1.31	0.59
$\|\Delta\|$ (%)	14.93	7.79		11.38	5.79

For comparison, second-order Møller-Plesset perturbation theory (MP2), coupled-cluster singles doubles (CCSD), and coupled-cluster singles doubles with single, double, and perturbative triple excitations [CCSD(T)] calculations were done for the set of small molecules from the first column of Table I. The CCSD(T) method serves as an accurate reference method in this work. In the case of the S22 dimer systems, the complete basis set (cbs)–extrapolated MP2 and CCSD(T) values were taken from the work of Takatani *et al.* [41]. In the case of the potential energy curves of the C_2H_4-C_2H_2 dimer and the C_2H_4 dimer, F12-MP2, F12a-CCSD, and F12a-CCSD(T) [42–44] calculations have been performed for comparsion.

All correlation energies have been extrapolated to the cbs limit by using the two-point extrapolation formula from Bak *et al.* [45] using correlation energies calculated with the augmented valence triple-zeta (aug-cc-pVTZ) and quadruple-zeta (aug-cc-pVQZ) basis set by Dunning [46]. The reference energies have not been extrapolated but were calculated using the aug-cc-pVQZ basis set, which yields reference energies with a negligible basis set error.

In the case of the explicitly correlated F12 methods, the aug-cc-pVDZ basis set has been employed. Since the use of this basis set in explicitly correlated calculations generally gives correlation energies smaller on magnitude than corresponding basis set extrapolated values, the F12a model was used, as this is known to yield results slightly overestimating the cbs limit results if large basis sets are used. Moreover, the triples correction was calculated without using F12 terms and therefore has been scaled by the ratio $E_c^{\mathrm{MP2-F12}}/E_c^{\mathrm{MP2}}$ as proposed and tested in [44] with $E_c^{\mathrm{MP2-F12}}$, E_c^{MP2} being the correlation energies of MP2-F12 and MP2, respectively. The CABS (complementary auxiliary basis set) singles correction was included in the reference energy as proposed in Refs. [42,43]. It has been found that at the equilibrium distances of C_2H_4-C_2H_2 and $(C_2H_4)_2$ the thus-obtained F12 results are close to the basis set extrapolated interaction energies of Takatani *et al.* [41].

In calculations with more than 400 basis functions, density fitting has been employed to calculate the molecular repulsion integrals. In the case of the Coulomb and exchange integrals, the aug-cc-pVXZ-JKFit ($X = D,T,Q$) fitting basis set of Weigend [47] has been used with X corresponding to the cardinal number of the orbital basis set. For the correlation calculations, the density fitting approach [Eq. (5)] was used unless otherwise noted. For this, the aug-cc-pVXZ-MP2fit basis set from Weigend *et al.* [48] has been used, again with X corresponding to the respective orbital basis.

Since the current implementation of the RPAX2 method has not yet been fully optimized, here only a few details of the timing for one larger system are given: for the stacked form of the uracil dimer using the aug-cc-pVQZ orbital basis set (1648 basis functions), a processing time of 24 min per iteration has been measured on a 3-GHz Intel Woodcrest machine. Compared to this, a corresponding density fitting MP2 calculation [49] for this system required only 12 min on the same computer. The main reason for the larger processing time (per cycle) of the RPAX2 method compared to DF-MP2 is that in addition to the generation of the amplitudes, Eq. (17), also a contraction of the amplitudes with the three-index $\mathbf{L}$ matrix is required in each iteration cycle; see Eq. (18). The computational cost for this step is about the same as for the generation of the amplitudes and thus explains the timing difference to the DF-MP2 method. Furthermore, note that while for the systems studied in this work the three-index matrices $\mathbf{U}^{(n)}$ could be kept in memory, this will not be possible anymore for even larger systems, so these then have to be written on disk, slowing down the real computation time.

Core electrons have been kept frozen in the calculations. The Boys-Bernadi counterpoise correction [50] was used in the intermolecular interaction energy calculations in order to reduce the basis set superposition error (BSSE). All calculations were done using the developers version of the MOLPRO quantum chemistry program [51].

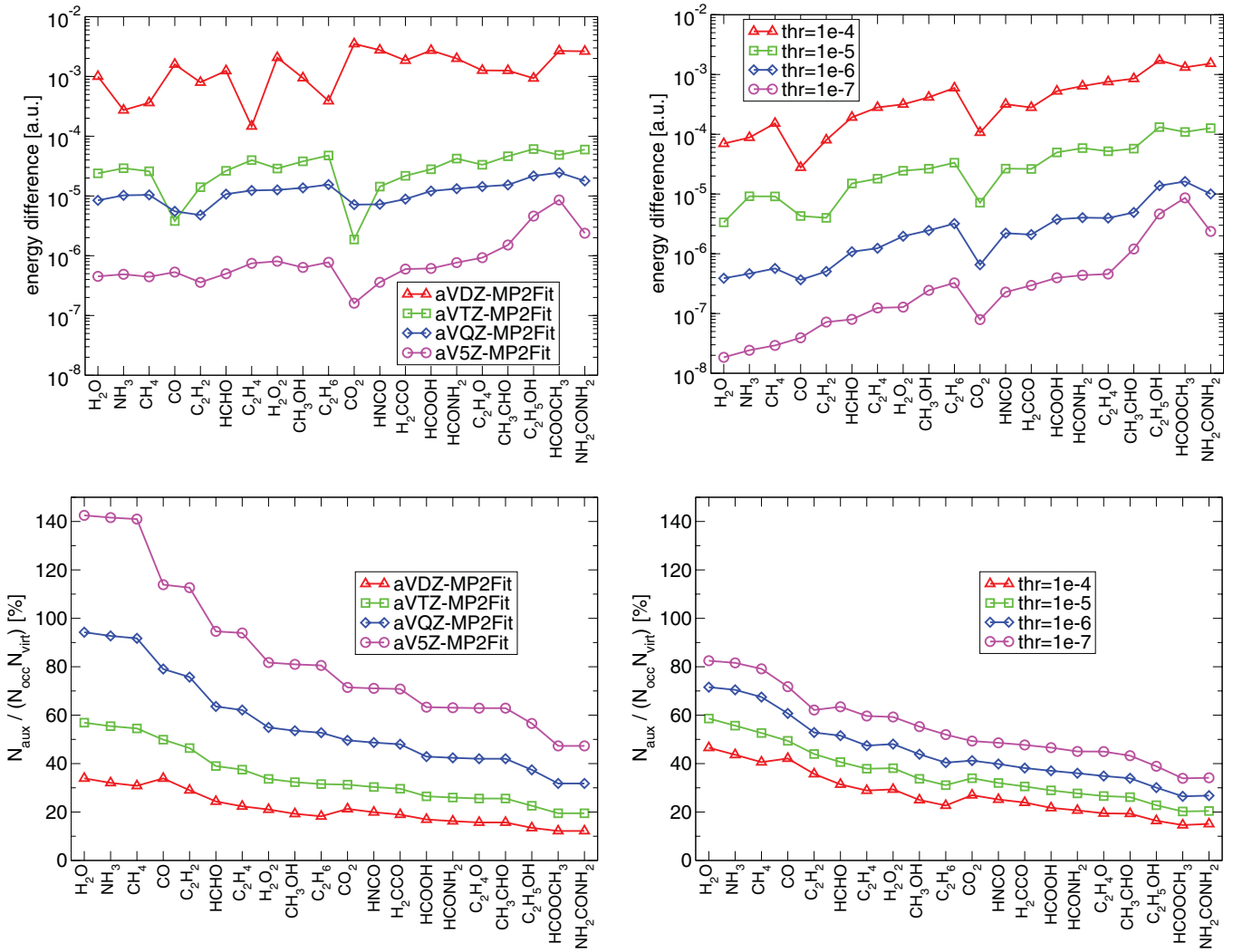

FIG. 2. (Color online) Absolute deviations of RPAX2 energies using density fitting (top left) or Cholesky decomposition (top right) from numerically exact RPAX2 energies in the aug-cc-pVTZ orbital basis set. The bottom diagrams show the ratio of the number of auxiliary functions (left) or Cholesky vectors (right) N_{aux} over the number of occupied times virtual orbitals $N_{\text{occ}} \times N_{\text{virt}}$.

IV. RESULTS

A. Accuracy of total energies using the C matrix decomposition

The two diagrams in the top of Fig. 2 show the numerical accuracy of the RPAX2 energy [Eq. (19)] calculated with the aug-cc-pVTZ orbital basis set for various small molecules using the decompositions of Eqs. (5) and (4). In case of the density fitting decomposition (left top diagram in Fig. 2), the aug-cc-pVXZ-MP2Fit basis sets [48] were used as auxiliary basis with $X = D,T,Q,5$. It can be observed that the error clearly decreases when increasing the auxiliary basis set size from double to quintuple-ζ quality. However, this decrease is irregular as one can see a large decrease from aVDZ→aVTZ and a notable decrease from aVQZ→aV5Z while the decrease from aVTZ→aVQZ is rather small, and sometimes the aVQZ fitting basis set even yields energies that more strongly deviate from the exact energy than the aVTZ basis set. In contrast to this, the energy errors for the Cholesky decomposition approach, which is simply controlled using a threshold value for the linear dependence of the Cholesky vectors, behave more regular with increasing auxiliary basis set size (here corresponding to the number of nonlinearly dependent Cholesky vectors). This can be seen in the top right diagram in Fig. 2, which shows the errors for Cholesky thresholds of 10^{-4}, 10^{-5}, 10^{-6}, and 10^{-7}. On the other hand, it appears that the error of the RPAX2 energies using the Cholesky decomposition become larger with increasing system size (left → right in the diagrams) while with the density fitting approach the errors seem to be less dependent on the system size. Another important result of this analysis is that the aVTZ-MP2Fit auxiliary basis set, which corresponds to the orbital basis with respect to the cardinal number, yields errors that are smaller than 10^{-4} hartree. This is lower than 0.1 kcal/mol and therefore should give sufficient accuracy in most applications. In the case of the Cholesky decomposition approach, this accuracy is achieved if the Cholesky threshold is at least set to a value of 10^{-5} or lower; see the top right diagram in Fig. 2.

In the two bottom diagrams of Fig. 2, the percentage contribution of the number of auxiliary functions used in

the density fitting case (left) and the Cholesky decomposition case (right) to the total number of occupied times unoccupied orbitals, which is the dimension of the matrix **C**, are shown. As expected, a drastic reduction of the number of auxiliary functions required to decompose the matrix **C** is obtained upon increase of the system size (left → right in the diagrams). One can observe that the number of auxiliary functions with the density fitting aVTZ-MP2Fit basis set corresponds well with the number of Cholesky vectors with a Cholesky threshold of 10^{-5} for the different molecules. This explains why in both cases the deviations to the exact energies are comparable.

B. Total energies

In Fig. 3, the energy differences of MP2, CCSD, RPAX, and RPAX2 to CCSD(T) total energies are shown for some small organic molecules. Note that the molecules on the abscissa are ordered with respect to the absolute value of the total CCSD(T) energy so that the order is approximately from small to larger systems in the diagram. It can be seen that with only few exceptions all methods yield energies that underestimate the CCSD(T) energies; that is, the energies usually are higher than with CCSD(T). The MP2, CCSD, and RPAX methods yield total energies which have similar deviations to the CCSD(T) energies; however, in the case of MP2 the deviations behave very irregularly upon increase of the system size. In contrast to this, the deviations of the CCSD and RPAX energies to CCSD(T) are more regular and tend to become larger in magnitude for the larger molecular systems. Also note that both the CCSD and RPAX energies are quite close to each other for the systems shown in Fig. 3. Clearly smaller deviations to the CCSD(T) energies are obtained with the RPAX2 method that yields energies which do not deviate by more than 0.015 hartree for the molecular systems considered, while in the case of CCSD and RPAX the maximal deviation found is about 0.04 hartree. Also, the diagram in Fig. 3 shows that the deviations of the RPAX2 energies behave rather regularly when increasing the system size; that is, the deviation to the CCSD(T) energies gradually increases for the larger molecules. In Sec. IV C, we investigate whether this finding also plays a role for molecular reaction energies calculated from the total energies of the molecules of Fig. 3.

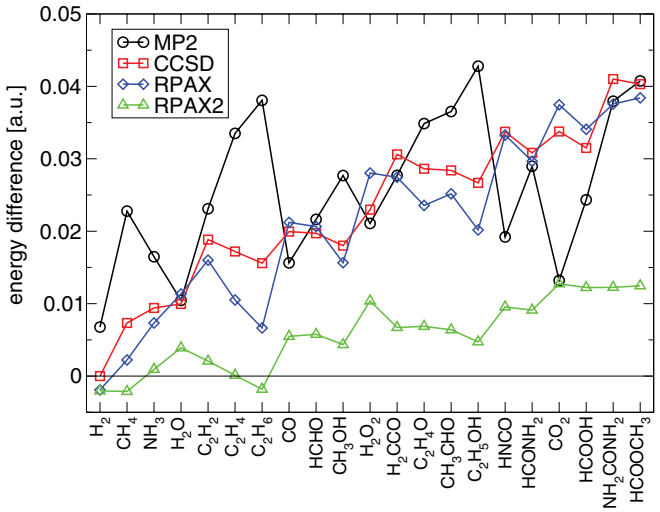

FIG. 3. (Color online) Energy differences of various methods to CCSD(T) energies. All energies are extrapolated to the complete basis set limit.

C. Reaction energies

Table I displays the reaction energies for various methods for the set of chemical reactions shown in the first column of the table. One can observe that the reaction energies yielded by the CCSD method are, with few exceptions, consistently closer to the CCSD(T) reference values than the MP2 reaction energies, as expected. The mean absolute error (mae) for the CCSD method is about 1 kcal/mol only for the reactions shown and thus only one half of the error of MP2; see the statistical data in the last two lines in the table. In comparison to this, the RPAX reaction energies are also closer to the CCSD(T) values than the MP2 reaction energies, but the improvement is not as large as with CCSD. More precisely, the mean absolute error of RPAX for the set of chemical reactions is 1.31 kcal/mol and thus about 0.35 kcal/mol larger than with CCSD. The absolute percentage error of RPAX, which is more biased to measure the errors of chemical reactions with a smaller reaction energy, is 11.4% and thus clearly larger than the deviation of 7.8% yield by CCSD. In contrast to this, the reaction energies of the RPAX2 method are more close to the CCSD(T) reaction energies than the CCSD reaction energies. The mean absolute error of RPAX2 is 0.6 kcal/mol only and thus almost only half as large as with CCSD. Also, the absolute percentage error of RPAX2 is smaller by 2% on average than with CCSD, though for this measure the improvement is not as large due to a relatively large error for the $CO+H_2 \rightarrow HCHO$ reaction of about 30% of the RPAX2 method, which is the only significant outlier for the given test set. From this finding it can be concluded that the good performance of the RPAX2 methods for total energies as observed in Sec. IV B also transfers to some extent to its ability to predict reaction energies with good accuracy.

D. Intermolecular interaction energies

The S22 database of intermolecular complexes developed by Hobza *et al.* [39] has emerged as a standard test set for assessing new methods for their ability to describe intermolecular interaction energies. It comprises seven hydrogen-bridged, eight dispersion-dominated, and seven mixed-type dimer complexes in their equilibrium structure (see Table II) and thus presents a challenging test for quantum chemistry methods that often yield an unbalanced description for the different interaction types. One example for this is the MP2 method, which shows very good performance for hydrogen-bridged systems (see lines 1–7 in Table II), while its accuracy strongly deteriorates compared to CCSD(T) interaction energies for dispersion-dominated systems (see lines 8–15 in Table II). In total, the MP2 method yields an error of 0.88 kcal/mol to the CCSD(T) reference interaction energies for the S22 database, which is unacceptably large for studying weak interactions of molecules.

In Table II, only interaction energies yielded by the RPAX2 method are shown, not those for the RPAX method. The reasons for this are that the scheme for calculating RPAX energies cannot be cast in a computational efficient approach as with RPAX2—see Sec. II B—so that the calculation of

TABLE II. Intermolecular interaction energies for the S22 complexes (in kcal/mol). The mean absolute errors (mae) and relative deviations (|Δ|) to the CCSD(T) reference values are shown in the last two lines of the table.

Dimer	MP2/cbs	CCSD(T)/cbs	RPAX2 aVDZ→aVTZ	RPAX2 aVTZ→aVQZ
$(NH_3)_2$ (C_{2h})	−3.16	−3.17	−2.94	−3.00
$(H_2O)_2$ (C_s)	−4.98	−5.02	−4.70	−4.83
$(HCOOH)_2$ (C_{2h})	−18.57	−18.80	−18.64	−19.13
$(CHONH_2)_2$	−15.84	−16.12	−16.09	−16.45
Uracil-uracil (C_{2h})	−20.41	−20.69	−20.89	−20.85
2-Pyridoxine-2-aminopyridine	−17.37	−17.00	−16.83	−17.13
AT (WC)	−16.54	−16.74	−16.61	−16.91
$(CH_4)_2$ (D_{3d})	−0.49	−0.53	−0.59	−0.59
$(C_2H_4)_2$ (D_{2d})	−1.58	−1.50	−1.58	−1.59
Bz-CH_4 (C_3)	−1.81	−1.45	−1.44	−1.47
Bz-Bz (C_{2h})	−4.96	−2.62	−2.32	−2.37
Pyrazine-pyrazine (C_s)	−6.91	−4.20	−3.79	−3.90
Uracil-uracil (C_2)	−11.10	−9.74	−9.87	−10.04
Indole-Bz (stacked)	−8.09	−4.59	−3.99	−4.08
AT (stacked)	−14.83	−11.66	−11.29	−11.51
C_2H_4-C_2H_2 (C_{2v})	−1.67	−1.51	−1.52	−1.53
Bz-H_2O (C_s)	−3.54	−3.29	−3.28	−3.33
Bz-NH_3 (C_s)	−2.66	−2.32	−2.33	−2.37
Bz-HCN (C_s)	−5.16	−4.55	−4.43	−4.50
Bz-Bz (C_{2v})	−3.63	−2.71	−2.69	−2.72
Indole-Bz (T-shaped)	−6.98	−5.62	−5.63	−5.68
Phenole-phenole	−7.76	−7.09	−6.96	−7.12
mae (total)	0.88		0.16	0.16
|Δ%| (total)	19.61		3.60	3.39

interaction energies for larger systems as the adenine-thymine base pair is prohibitively large, especially if large basis sets are used. Moreover, it has been observed for smaller dimer systems that, similar to the reaction energies–see Sec. IV C—the RPAX method yields worse results than RPAX2 if compared to CCSD(T) reference values. Because of this, here only the performance of the RPAX2 method is studied.

The RPAX2 interaction energies for the S22 systems are shown for two basis set extrapolation schemes in the columns 4 and 5 in Table II, namely using an aVDZ→aVTZ extrapolation and an aVTZ→aVQZ extrapolation. As can be seen, with exception of the strong hydrogen-bridged sytems $(HCOOH)_2$ and $(CHONH_2)_2$, the aVDZ→aVTZ extrapolation yields interaction energies that deviate by only +0.1 to +0.2 kcal/mol to the aVTZ→aVQZ extrapolated results. This means that in most cases it suffices to do calculations with the moderately large aug-cc-pVTZ basis set only in order to obtain extrapolated results that are fairly converged.

The average absolute error of 0.16 kcal/mol of the RPAX2 interaction energies shown in Table II indicates not only a large improvement over the MP2 interaction energies but also such high accuracy that has not been observed even for a number of recently developed (partially semiempirical) density functional [52–57] and wave function methods [21,41,58,59]. In fact, with exception of the semiempirical double hybrid functional B2PLYP-D, for which even a mean absolute deviation of only 0.12 kcal/mol is reported [41], to the best of our knowledge, no other quantum chemistry method tested so far for the S22 dimer systems has yielded such a small error to the CCSD(T) reference interaction energies. An analysis of the errors for the individual interaction-type groups of the S22 database yields errors of 0.23 kcal/mol for the hydrogen-bridged systems and 0.26 kcal/mol for the dispersion-dominated systems for RPAX2. This shows that the method gives a very balanced description for these different interaction types. In the case of the mixed-type systems, an error of only 0.04 kcal/mol to the coupled-cluster reference values is obtained.

It should be noted that this good performance of the RPAX2 method to some extent depends on the reference determinant used. Some of the smaller systems of the S22 database, namely $(H_2O)_2$, $(NH_3)_2$, $(CH_4)_2$, $(C_2H_4)_2$, and C_2H_4-C_2H_2, were also calculated using the full PBE functional instead of the exchange-only PBEx functional for calculating the reference determinant. It has been observed that on average the interaction energies yield by RPAX2 based on the PBE determinant decreases by about 0.2 kcal/mol in magnitude and thus worsens the results shown for the PBEx case in Table II. This shows that even the choice of different GGA functionals for calculating the reference determinant matters in this case and should be investigated further in future works. Note that a corresponding study for the reaction energies did not show such a significant dependence of the reference determinant on the performance of the method, apparently because here the total energy differences are larger on average; see Table I.

Since the S22 dimer systems comprise only equilibrium structures, the RPAX2 method has also been tested at nonequilibrium dimer configurations for two systems from

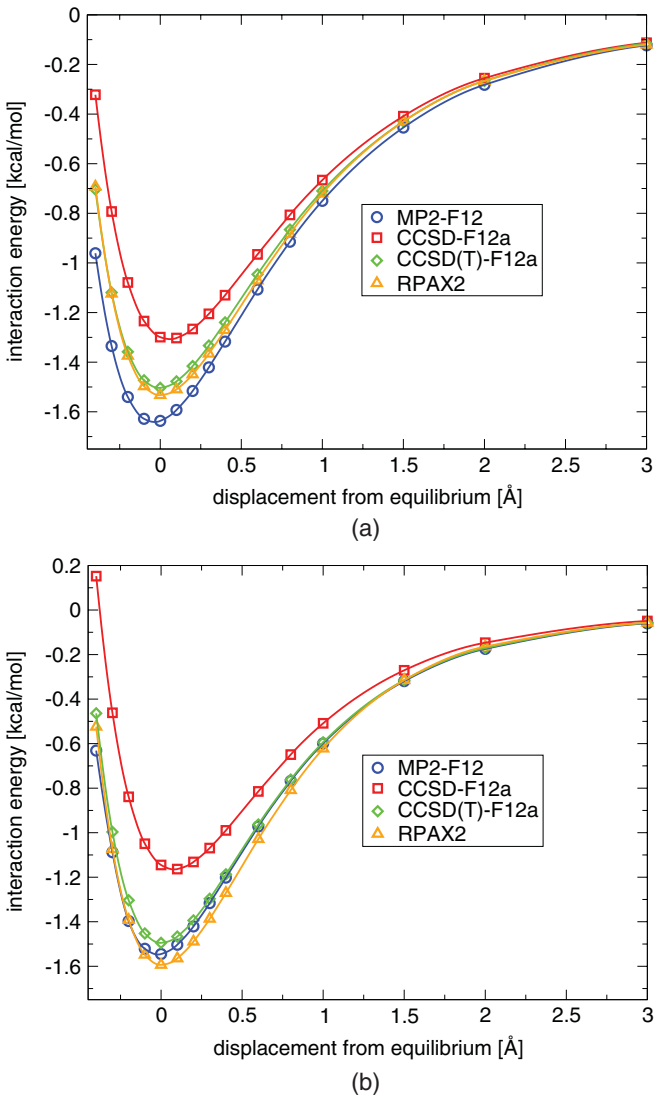

FIG. 4. (Color online) Interaction energy potentials for the ethylene-acetylene (top) and ethylene dimer (bottom).

the S22 set, namely the ethene-ethyne dimer, which belongs to the mixed-type complexes, and the ethene dimer, which is categorized as a dispersion-dominated system. The potential energy curves of RPAX2 and CCSD(T) along with MP2 and CCSD curves for both systems are shown in Fig. 4 (refer to Sec. III for details). Note that the far asymptotic region is not shown in both cases, as in this region all curves are indistinguishable. In the case of the C_2H_4-C_2H_2 dimer, Fig. 4(a), one can observe that MP2 slightly overestimates and CCSD underestimates the CCSD(T) interaction curve at short and close equilibrium distances. In contrast to this, the RPAX2 interaction potential is very close to the CCSD(T) potential for all distances shown in the diagram. This is different in the case of the C_2H_4 dimer, where in the minimum region the RPAX2 method yields interaction energies slightly larger than with CCSD(T) while interestingly here the MP2 curve follows the CCSD(T) curve more closely. In both cases, for C_2H_4-C_2H_2 and $(C_2H_4)_2$ the locations of the potential minima yield by the different methods agree well with each other. The largest deviation to the locations of the CCSD(T) minima is found for CCSD with displacements of +0.070 Å and +0.090 Å for C_2H_4-C_2H_2 and $(C_2H_4)_2$, respectively. Compared to this, for RPAX2 displacements smaller than 0.01 Å from the CCSD(T), equilibrium are found.

V. SUMMARY

Two new random-phase approximation (RPA) correlation methods have been developed which take into account exchange effects, termed as RPAX and RPAX2. Both methods are based on a modified ring coupled-cluster doubles amplitude equation in which all integrals are replaced by antisymmetrized integrals; see Eq. (11). This modification has been justified with the fact that the correlation energy calculated using the solutions of the amplitude equation correspond to the EXX-RPA correlation energy for two-electron systems. However, while exact to second-order of perturbation theory, it has been observed that the first method obtained in this way, termed RPAX, yields third-order correlation contributions which do not correspond to proper perturbation theory diagrams. A simple modification of the amplitude equation by replacing the antisymmetrization operator could solve this problem and at the same time has lead to a computationally efficient scheme that scales only with the fifth power of the molecular size with the aid of density fitting or the Cholesky decomposition. This second approach, termed RPAX2, is therefore applicable to fairly large molecular systems for which also standard (density fitting) second-order Møller-Plesset perturbation (MP2) theory methods are still feasible.

In this work, the reference determinant used in the RPAX and RPAX2 method has been obtained from a preceding Kohn-Sham DFT calculation using the PBE exchange functional. It has been argued that the similarity of Kohn-Sham orbitals and Brueckner orbitals from a Brueckner coupled-cluster wave function means that in this way the approach is able to capture single excitations which are not described in standard RPA methods. It has been observed that especially for weak intermolecular interactions the choice of the density functional plays a role; for example, when using the full PBE functional, the intermolecular interaction energy results with the RPAX2 method deteriorate.

The numerical accuracies of the density fitting and the Cholesky decomposition methods have been tested for a number of small molecules using the aug-cc-pVTZ orbital basis set. It has been found that in the density fitting case the corresponding aug-cc-pVTZ-MP2Fit auxiliary basis set is sufficient to obtain errors lower than 0.1 kcal/mol, which is good enough in most practical applications. Correspondingly, using the Cholesky decomposition, a threshold of 10^{-5} turned out to be sufficient to obtain total energies of 0.1 kcal/mol accuracy and lower.

Numerical tests on reaction energies and intermolecular interaction energies revealed a moderate good performance for the RPAX method and an extremely good performance for the RPAX2 method. For the small test set of organic reactions, the RPAX method performed better than the MP2 method but not as well as CCSD if compared to CCSD(T) reference results. In contrast to this, the RPAX2 method yielded a mean absolute error of 0.6 kcal/mol only for the chemical reactions considered, almost reducing the error of

the CCSD method by one half. For the S22 database, a very small average absolute error of 0.16 kcal/mol was found for the RPAX2 method, which is surprisingly accurate for a method that is free from any empirical parameters as compared to other recent correlation methods that aim at describing weak intermolecular interactions [21,41,52–59]. The study of the C_2H_4-C_2H_2 and the $(C_2H_4)_2$ dimers at nonequilibrium intermolecular distances has shown that in the asymptotic short- and long-range parts of the intermolecular interaction potentials the RPAX2 interaction energies are quantitatively in agreement with CCSD(T) reference interaction energies. Further tests, however, are required for a full assessment.

[1] R. D. Mattuck, *A Guide to Feynman Diagrams in the Many-Body Problem* (Dover, New York, 1992).
[2] M. Hellgren and U. von Barth, J. Chem. Phys. **132**, 044101 (2010).
[3] A. Heßelmann, J. Chem. Phys. **134**, 204107 (2011).
[4] A. Heßelmann and A. Görling, Mol. Phys. **109**, 2473 (2011).
[5] A. D. MacLachlan and M. A. Ball, Rev. Mod. Phys. **36**, 844 (1964).
[6] N. Fukuda, F. Iwamoto, and K. Sawada, Phys. Rev. **135**, A932 (1964).
[7] A. Szabo and N. S. Ostlund, J. Chem. Phys. **67**, 4351 (1977).
[8] A. Szabo and N. S. Ostlund, Int. J. Quant. Chem. **S11**, 389 (1977).
[9] J. Oddershede, Adv. Quant. Chem. **11**, 275 (1978).
[10] H. Jiang and E. Engel, J. Chem. Phys. **127**, 184108 (2007).
[11] A. Grüneis, M. Marsman, J. Harl, L. Schimka, and G. Kresse, J. Chem. Phys. **131**, 154115 (2009).
[12] M. J. Packer, E. K. Dalskov, T. Enevoldsen, H. J. A. Jensen, and J. Oddershede, J. Chem. Phys. **105**, 5886 (1996).
[13] J. Toulouse, I. C. Gerber, G. Jansen, A. Savin, and J. G. Angyan, Phys. Rev. Lett. **102**, 096404 (2009).
[14] F. Furche, Phys. Rev. B **64**, 195120 (2001).
[15] F. Furche, J. Chem. Phys. **129**, 114105 (2008).
[16] J. Harl, L. Schimka, and G. Kresse, Phys. Rev. B **81**, 115126 (2010).
[17] J. Angyan, R.-F. Liu, J. Toulouse, and G. Jansen, J. Chem. Theory Comput. **7**, 3116 (2011).
[18] B. G. Janesko, T. M. Henderson, and G. E. Scuseria, J. Phys. Chem. **130**, 081105 (2009).
[19] B. G. Janesko, T. M. Henderson, and G. E. Scuseria, J. Phys. Chem. **131**, 034110 (2009); **133**, 179901(E) (2010).
[20] J. Paier, B. G. Janesko, T. M. Henderson, G. E. Scuseria, A. Grüneis, and G. Kresse, J. Chem. Phys. **132**, 094103 (2010); **133**, 179902(E) (2010).
[21] J. Toulouse, W. Zhu, A. Savin, G. Jansen, and J. G. Angyan, J. Chem. Phys. **135**, 084119 (2011).
[22] M. Hellgren and U. von Barth, Phys. Rev. B **78**, 115107 (2008).
[23] A. Heßelmann and A. Görling, Mol. Phys. **108**, 359 (2010).
[24] A. Heßelmann and A. Görling, Phys. Rev. Lett. **106**, 093001 (2011).
[25] F. E. Harris, H. J. Monkhorst, and D. L. Freeman, *Algebraic and Diagrammatic Methods in Many–Fermion Theory* (Oxford, Oxford University Press, 1992).
[26] G. E. Scuseria, T. M. Henderson, and D. C. Sorensen, J. Chem. Phys. **129**, 231101 (2008).
[27] H. Eshuis, J. Yarkony, and F. Furche, J. Chem. Phys. **132**, 234114 (2010).
[28] G. Jansen, R.-F. Liu, and J. G. Angyan, J. Chem. Phys. **133**, 154106 (2010).
[29] E. A. Sanderson, Phys. Lett. **19**, 141 (1965).
[30] N. H. F. Beebe and J. Linderberg, Int. J. Quant. Chem. **12**, 683 (1977).
[31] I. Røggen and T. Johansen, J. Chem. Phys. **128**, 194107 (2008).
[32] E. J. Baerends, D. E. Ellis, and P. Ros, Chem. Phys. **2**, 41 (1973).
[33] J. L. Whitten, J. Chem. Phys. **58**, 4496 (1973).
[34] O. Vahtras, J. Almlöf, and M. W. Feyereisen, Chem. Phys. Lett. **213**, 514 (1993).
[35] H. Koch and A. Sanchez de Meras, J. Chem. Phys. **113**, 508 (2000).
[36] A. Heßelmann, Ph.D. thesis, Universität Duisburg-Essen, 2003 (unpublished).
[37] C. Hampel and H.-J. Werner, J. Chem. Phys. **104**, 6286 (1996).
[38] J. P. Perdew, K. Burke, and M. Ernzerhof, Phys. Rev. Lett. **77**, 3865 (1996).
[39] P. Jurečka, J. Šponer, J. Černý, and P. Hobza, Phys. Chem. Chem. Phys. **8**, 1985 (2006).
[40] H.-J. Werner, T. B. Adler, and F. R. Manby, J. Chem. Phys. **126**, 164102 (2007).
[41] T. Takatani, E. G. Hohenstein, M. Malagoli, M. S. Marshall, and C. D. Sherrill, J. Chem. Phys. **132**, 144104 (2010).
[42] T. B. Adler, G. Knizia, and H.-J. Werner, J. Chem. Phys. **127**, 221106 (2007).
[43] G. Knizia and H.-J. Werner, J. Chem. Phys. **128**, 154103 (2008).
[44] G. Knizia, T. B. Adler, and H.-J. Werner, J. Chem. Phys. **130**, 054104 (2009).
[45] K. L. Bak, P. Jørgensen, J. Olsen, T. Helgaker, and W. Klopper, J. Chem. Phys. **112**, 9229 (2000).
[46] T. H. Dunning, J. Chem. Phys. **90**, 1007 (1989).
[47] F. Weigend, Phys. Chem. Chem. Phys. **4**, 4285 (2002).
[48] F. Weigend, A. Köhn, and C. Hättig, J. Chem. Phys. **116**, 3175 (2002).
[49] H.-J. Werner, F. R. Manby, and P. J. Knowles, J. Chem. Phys. **118**, 8149 (2003).
[50] S. F. Boys and F. Bernadi, Mol. Phys. **19**, 553 (1970).
[51] H.-J. Werner and P. J. Knowles [http://www.molpro.net].
[52] T. Sato, T. Tsuneda, and K. Hirao, J. Chem. Phys. **126**, 234114 (2007).
[53] T. Sato and H. Nakai, J. Chem. Phys. **131**, 224104 (2009).
[54] A. Gulans, M. J. Puska, and R. M. Nieminen, Phys. Rev. B **79**, 201105(R) (2009).
[55] O. A. Vydrov and T. Van Voorhis, J. Chem. Phys. **132**, 164113 (2010).
[56] S. Grimme, J. Antony, S. Ehrlich, and H. Krieg, J. Chem. Phys. **132**, 154104 (2010).
[57] L. Burns, A. Vazquez-Mayagoitia, B. G. Sumpter, and C. D. Sherrill, J. Chem. Phys. **134**, 084107 (2011).
[58] O. Marchetti and H.-J. Werner, J. Phys. Chem. A **113**, 11580 (2009).
[59] M. Pitonak and A. Heßelmann, J. Chem. Theory Comput. **6**, 168 (2010).